A RESONANT BEAM DETECTOR FOR TEVATRON TUNE MONITORING

D. Martin, B. Fellenz, C. Hood, M. Johnson, R. Shafer, R. Siemann, J. Zurawski

Fermi National Accelerator Laboratory*
P.O. Box 500 Batavia, Il. 60510

Abstract

An inductively resonated, balanced stripline pickup has been constructed for observing tune spectra. The device is a sensitive betatron oscillation and Schottky noise pickup, providing 25 dB gain over untuned detectors of like geometry. The electrodes are motorized so the device center and aperture may be remotely adjusted. To tune the resonator onto the 21.4 MHz operating frequency, a motorized capacitor is employed. Quadrature signals from a pair of detectors has enabled observation of individual p and $\bar{p}$ coherent motions to nanometer levels.

Introduction

The Schottky signals of bunched beam currents are weak signals which recur at intervals of the revolution frequency. Detecting these signals with reasonable signal-to-noise ratio and small intermodulation effects of the coherent revolution lines suggests a narrowband beam pickup. From a system point of view, considering detector, amplifier, and processing electronics, the detector sensitivity, S_Λ, defines system signal-to-noise ratio. For an unbunched beam the ratio may be expressed

$$(S/N) = \frac{ef_o \sigma_\beta S_\Lambda \sqrt{N}/\sqrt{\Delta f}}{\sqrt{2RkT}} \qquad (1)$$

where f_o= revolution frequency, N= number of particles, σ_β= beam size from betatron oscillations, Δf= Schottky bandwidth[1]= $f_o(\Delta p/p)[(h\pm Q)\eta \pm \xi]$, R= load resistance and T= 290°K. An example using typical values (f_o= 47.7 kHz, N= 6E10, σ_β= .5 mm, Δf= 100 Hz, S_Λ= 35 Ω/mm, R= 50 Ω) gives 3.3 nV signal and (S/N)= 14 dB. Using Eqn. 2, an rms beam motion[2]

$$x_{rms} = \frac{rms}{S_\Lambda} \cdot \frac{---}{Nef_o} \qquad (2)$$

of .2 nm is found. The critical parameters for a Schottky pickup are thus sensitivity and narrow bandwidth. If a particle beam may be considered a current source, sensitivity is enhanced by raising the detector shunt impedance. High RF impedance and narrow bandwidth are each achieved by a high-Q circuit. No less important in the detector is the need to vary aperture- small when great sensitivity is desired, large for accelerator fixed target operation. Because Schottky signals are weak, shielding from external RF fields needs to be excellent. A means of remotely tuning the detector, to maintain resonant frequency as aperture changed, was an essential requirement. To verify resonant frequency, each detector was fitted with a -100 dB input for testing, calibration, and a process we call "autotuning".

Detector Description

Figure 1 is an oblique view of the Schottky detector. The one meter electrode length represented a compromise between beam interaction length and available beam line space. This length also allows the

horizontal and vertical pairs of detectors to be interleaved. Since orthogonal construction simplified the plate motion apparatus, the vacuum chamber was made 6 in. square cross section.(See Fig.2.) The chamber material is 1/4 in. thick 304 stainless steel, chosen for its rigidity and good vacuum properties. Because the signal energy is largely confined near the flat copper electrodes, an early concern that a stainless cavity would make the resonator lossy proved unfounded. Calculation and measurements showed the degradation to be 2% that of a silver enclosure, making the worst assumptions. (The dominant loss in the resonator is the inductor).
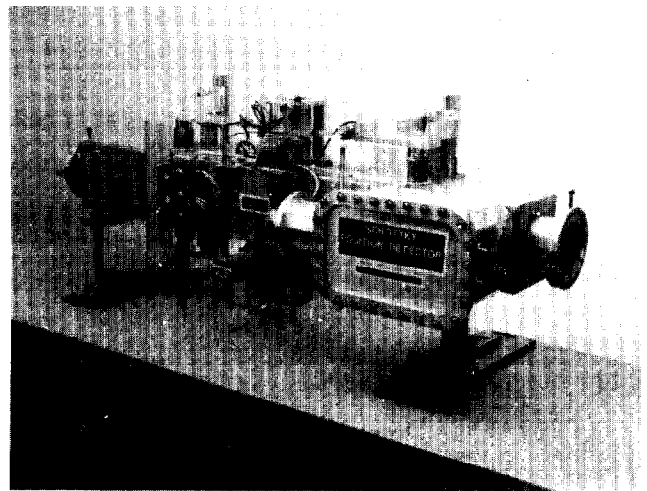

Figure 1.

To obtain signal orthogonality, skew and twisting of the 2 in. wide copper bars was specified below .005 in. Planing on both sides and stress relieving helped prevent warping. To position the electrodes, external motorized mechanisms are used. Each side has a stepping motor, with a worm gear on its drive shaft. The associated worm wheel is attached to a ball screw shaft, where the screw nut is fixed to a long aluminum bar that, through ceramic isolators (R_{RF} ~600 KΩ, C ~10 pF) and metal bellows, moves the copper bars as the aluminum bar moves on the ball screw. Linear ball slides guide the aluminum bars ensuring smooth motion. Limit switches are mounted to the box to prohibit the electrodes from colliding with each other or the vacuum chamber, and LVDT's provide electrode position readback.

The inductor, consisting of two turns 1/2 in. dia. copper tubing on a 2 in. radius, increases the electrical length of the plates for resonance at 21.4 MHz. It is also the primary of the output coupling transformer. The transformer secondary is .25 in. dia. copper coax with the outer conductor fashioned as a reentrant electrostatic shield. The transformer is thus sensitive only to magnetic flux, in effect making the electrical and mechanical detector centers coincident, all else being symmetric. For signal feedthroughs we selected copper, high current rated types to achieve low loss. To obtain maximum power transfer (critical coupling), the position of the output loop is carefully set during

final assembly. Since this condition could be obtained for only one plate gap, we chose .50 in., obtaining $Q_L = Q_o/2 = 370$. Located within the inductor housing is a 7-100 pF air variable trim capacitor, which keeps the detector on frequency for plate spacing between .28 in. and 2.5 in. Put another way, the device may be tuned from 16.5 MHz to 33.0 MHz.

To function in the accelerator environment EMI shielding needed to be exceptional. We therefore aspired to make the entire detector vacuum tight (or carefully design any leaks), since as a rule, a vacuum tight container will be RF tight, skin depth excepted. The beam enclosure by necessity is vacuum tight. To allow the inductor housing to be removed without violating our requirement, a copper C-seal was used between boxes. The access panel on the housing has a similar seal. No conductor penetrates the inductor housing ungrounded. All metal-to-metal joints were tested with a 1 A RF current. Running the test current from flange to flange over the detector body showed a leak of -145 dB.
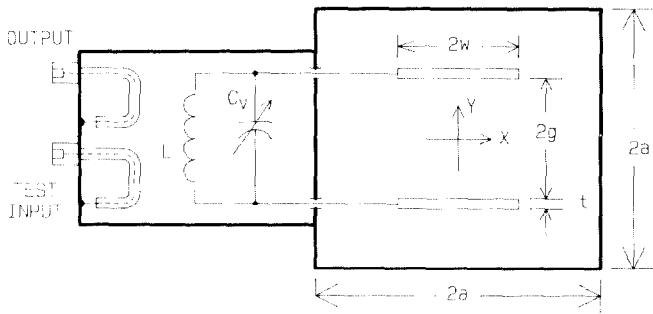

Fig. 2 Transverse Geometry

Detector Modeling

Electrical behavior of the device may be studied from the circuit models of Fig. 3. In the lumped element approximation[3], the two electrodes constitute a parallel plate capacitor, and the overall capacitance is $C = C_{PP} + C_V + C_{PG}/2$. The beam is modeled by current sources, the downstream sources shifted in phase by the particle flight time. The transformer effective turns ratio, a, is adjusted so that $a^2 = 2R_{SH}/R_L$ for critical coupling. The function $\Lambda(y)$ is the geometric sensitivity factor[4] for y-axis position offsets (x=0), which near center may be linearized $\Lambda(y) = (1-y/g)/2$. Solving for the voltage appearing across the load, the sensitivity[5] in (Ω/m) is obtained.

$$S_\Lambda = \frac{t_o}{g} \sqrt{\frac{\omega_o R_L Q_o}{C} \frac{Q_L}{Q_o} (1 - \frac{Q_L}{Q_o})} \qquad (3)$$

with Q_L and Q_o the loaded and unloaded Q, respectively, and ω_o= resonant frequency, t_o= plate flight time, R_L= output load resistance.

The detector displays characteristics of a distributed circuit at higher beam frequency components and has been modeled as in Fig. 3b. The detector striplines form a three conductor TEM line, so the even (Z_{oe}) and odd (Z_{oo}) mode impedances are used[6]. Each plate has the propagation constant γ, length 1, and flight time $t_o = 1/c$. Additionally, the capacity of the inductor to its grounded environment must be considered. The winding is a helical transmission line with parameters Z_o, γ_1, and axial length l_1. From this model are calculated the broadband impedances $Z_{\|}(\omega)$ and $Z_{\perp}(\omega)$[7].
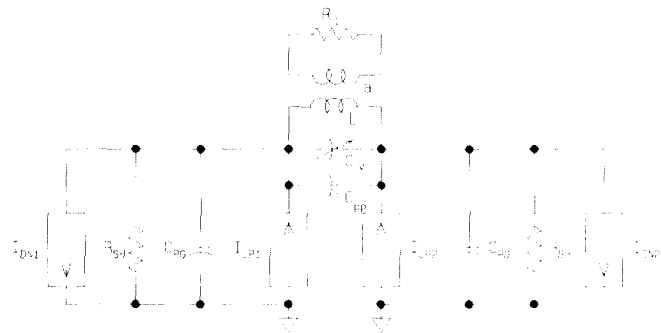

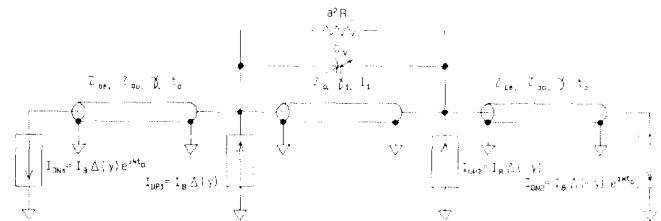Fig. 3a Lumped Element Equivalent Circuit

Fig. 3b Distributed Element Equivalent Circuit

Making certain approximations[8], the plate characteristic impedances are given by Eqn. 6. K is the complete elliptic integral of the first kind. The moduli k_o and k_e are related to the transverse dimensions by transcendental equations. By selecting permissible values of the moduli, geometrical ratios w/a and g/a are obtained, so that a family of impedance curves can be constructed. The impedances $Z_{\|}(\omega)$ and $Z_{\perp}(\omega)$ are plotted (Figs. 4,5) using the values a= 3 in., w= 1 in., g= .375 in., Z_{oe}= 212 Ω, Z_{oo}= 44 Ω, Z_o= 347 Ω, l= 1 m, l1= .2 m, v= c, v_1= .098c, a=1.05 E-5 $\sqrt{f}$, a_1= 5.72 E-5 $\sqrt{f}$, C_V= 0.

SCHOTTKY DETECTOR TRANSVERSE IMPEDANCE (MAGNITUDE) vs. N
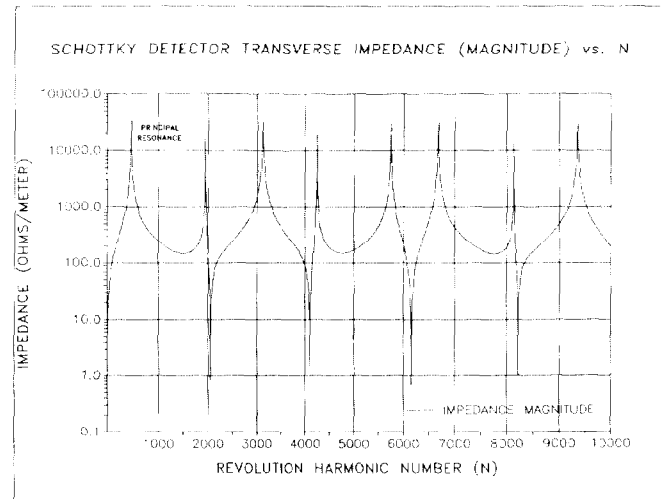
Figure 4.

Detector Tuning

The detector resonant frequency changes greatly with plate aperture, and means were required to monitor and remotely adjust it. Since the detectors are used only at 21.4 MHz, the task of tuning is

1487

simply to adjust C_V while measuring the developed signal when the detector is excited by a fixed test frequency. We established two modes of operation, the first called autotuning. In this mode, the capacitor is slowly rotated, beginning at an extreme of its range. The extreme is defined by a hard mechanical stop. To engage the stop without overloading the microstepping motor, the motor and capacitor are clutch connected. The clutch and hard stop provide a repeatable starting point from which motor steps may be counted, thus indexing the capacitor position. The test signal is monitored through the Schottky receiver[9] and peripheral electronics checks for a maximum response. Resolution is high (400 Hz/ motor step), and the electronics stops the capacitor at the peak response. This procedure is typically followed by manual tuning, in which the capacitor motor is moved a count or two in either direction. Either tuning operation may be controlled and monitored from an accelerator system console.
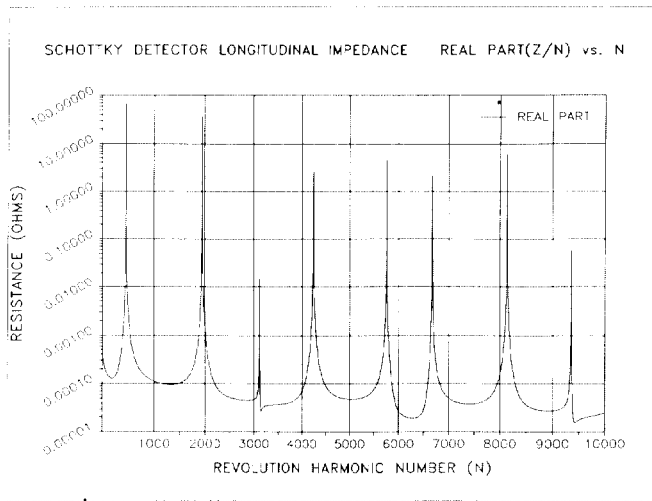
References

[1] D. Boussard, Schottky Noise and Beam Transfer Function Diagnostics, CERN SPS/86-11 (ARF) May, 1986.

[2] R. Siemann, Summary of Measurements of Betatron Line Amplitudes, RF Phase Noise, and Emittance Growth, Fermilab Note #EXP-155, May, 1987.

[3] D. Boussard, ibid.

[4] D. Neuffer, Calculation of Pick-up/Kicker Sensitivity, Fermilab P-bar Note #201, Feb. 1982.

[5] R. Siemann, ibid.

[6] G. Matthaei, L. Young, E.M.T. Jones, Microwave Filters, Impedance Matching Networks, and Coupling Structures, Artech, 1980., p. 174.

[7] D. Martin, Longitudinal and Transverse Impedances of an Inductively Resonated, Balanced Stripline Detector, Fermilab Note TM #1569, Dec. 1988.
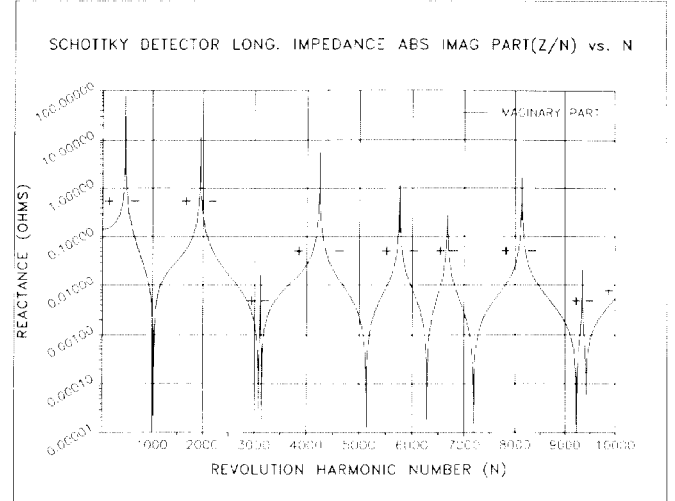
Figure 5a.

Figure 5b.

Acknowledgements

The authors would like to thank the many individuals who contributed to this equipment, and especially: Q. Kerns, for discussions on shielding and tuned detectors; G. Lee, for mechanical concepts; S. Lackey, for providing motion control support systems; and A. Beutler, J. Schmidt, and R. Franck for expert fabrication and assembly of the vacuum components.

[8] D. Martin, Even and Odd Mode Impedances of Thin, Broadside Coupled Plates Between Ground Planes, Fermilab Note TM #1570, March 1989.

[9] D. Martin et al., A Schottky Receiver for Non-Perturbative Tune Monitoring in the Tevatron, this Proceedings.

$$Z_\parallel(\omega) = \frac{Z_{oe}^2 \sinh\gamma l \, \sinh\gamma_1 l_1 + 2Z_o Z_{oe}(\cosh\gamma_1 l_1 - 1)(\cosh\gamma l - \cos\omega t_o)}{Z_{oe}\cosh\gamma l \, \sinh\gamma_1 l_1 + Z_o \sinh\gamma l \,(\cosh\gamma_1 l_1 - 1)} \tag{4}$$

$$Z_\perp(\omega) = \frac{Z_L Z_o Z_{oo}(\cosh\gamma_1 l_1 - 1)(e^{i\omega t}o + \cosh\gamma l)}{2Z_o Z_{oo}\cosh\gamma l \,(\cosh\gamma_1 l_1 - 1) + Z_L Z_{oo}\cosh\gamma l \, \sinh\gamma_1 l_1 + Z_L Z_o \sinh\gamma l \,(\cosh\gamma_1 l_1 - 1)} \, \Delta^*(y) \tag{5}$$

$$\Delta^*(y) = \frac{d}{dy}\,[\Delta(y) - \Delta(-y)] \qquad \Delta(y) = \frac{1}{\pi}\tan^{-1}\left[\frac{\sinh(\pi w/2g)}{\cos(\pi y/2g)}\right] + \frac{1}{\pi}\tan^{-1}\left[\tan\frac{\pi y}{2g}\tanh\frac{\pi w}{2g}\right]$$

$$Z_{oe} = \frac{1}{4}\frac{\sqrt{\mu_o}}{\sqrt{\epsilon_o}}\frac{K(k_e^*)}{K(k_e)} \qquad\qquad Z_{oo} = \frac{\sqrt{\mu_o}}{\sqrt{\epsilon_o}}\frac{K(k_o)}{K(k_o^*)} \tag{6}$$